EUROPEAN FUSION DEVELOPMENT AGREEMENT

EFDA–JET–CP(06)03-16

R. Sabot, F. Clairet, G.D. Conway, X. Garbet, G. Falchetto, T. Gerbaud,
S. Hacquin, P. Hennequin, S. Heuraux, C. Honoré, G. Leclert, A. Sirinelli,
L. Vermare, A. Truc and JET-EFDA Contributors

Recent Results on Turbulence and MHD Activity Achieved by Reflectometry

Recent Results on Turbulence and MHD Activity Achieved by Reflectometry

R. Sabot[1], F. Clairet[1], G.D. Conway[2], X. Garbet[1], G. Falchetto[1], T. Gerbaud[1], S. Hacquin[3], P. Hennequin[4], S. Heuraux[5], C. Honoré[4], G. Leclert[6], A. Sirinelli[1], L. Vermare[2], A. Truc[4] and JET-EFDA Contributors*

[1]Association Euratom-CEA, CEA/DSM/DRFC, CEA Cadarache, 13108 Saint Paul lez Durance, France
[2]Max-Planck-Institut f¨ur Plasmaphysik, EURATOM-Association IPP, D-85748 Garching, Germany
[3]Association Euratom CFN_IST, Av. Rovisco Pais, 1049-001 Lisboa, Portugal
[4]LPTP, CNRS (UMR-7648), Ecole Polytechnique, 91128 Palaiseau, France
[5]LPMIA, CNRS (UMR 7040) Université Henri Poincaré, BP 239, 54506 VANDOEUVRE Cedex, France
[6]LPIIM, CNRS (UMR 6633) - Université de Provence,13397 Marseille Cedex 20, France*JET Results and Future Perspectives",*
Fusion Energy 2000 (Proc. 18th Int. Conf. Sorrento, 2000), IAEA, Vienna (2001).

Preprint of Paper to be submitted for publication in Proceedings of the
33rd EPS Conference,
(Rome, Italy 19-23 June 2006)

ABSTRACT

Over the last years, help by the development of new methods and technical progresses, reflectometry diagnostics brought news results on transport, turbulence and MHD. Combining density profile and fluctuation measurement, it was shown on Tore-Supra that the particle pinch inside the q=1 surface is close to neo-classical value in ohmic plasma, while the observed small diffusion is in agreement with a very low level of density fluctuations inside the q=1 surface. In β scaling experiment, not change in the fluctuations levels was found, in agreement with the very weak confinement degradation with increasing β. Zonal flows have been detected by Doppler in Asdex-Upgrade and with correlation reflectometry in T-10. On Tore-Supra, a fast decrease of density fluctuation level at high poloidal wave number was measured with Doppler reflectometry, suggesting a minor role of Electron Temperature Gradient driven modes (ETG). Various forms of Alfvén eigen modes (TAEs, Alfvén Cascades, possibly BAEs) have been detected with reflectometry in JET and Tore-Supra, they present an anti ballooning profile.

1. INTRODUCTION

The understanding of turbulence and Magneto-Hydro-Dynamic (MHD) activity in magnetized plasmas is a key issue for a fusion reactor. The large heat and particle transport is attributed to drift wave turbulence destabilised by temperature and density gradients [1]. Although significant progress have been made [2], some issues are still unclear. In particular, the profile of density in ITER is still a subject of debate. With particle sources being localised in the outer part, an inward particles pinch is needed to built peaked profiles.

The energy confinement in ITER is predicted with scaling laws extrapolated from engineer parameters database. When rewritten with dimensionless parameters, large uncertainties remains on some parameter dependence like β, the ratio of plasma pressure to magnetic pressure. Confidence in ITER performances would also benefit from a better understanding of the role of zonal flows (ZF). The drift wave turbulence is though to create these zonal flows that in turn tend to stabilize the drift waves according to the new paradigm that was reviewed by P. Diamond et al [3]. Although this paradigm develops in nearly all cases of drift wave turbulence, it is still important to identify the underlying drift wave instability, in particular because in ITER, electron heating will be dominant. The most commonly invoked instabilities are ion temperature gradient (ITG) mode, the trapped electron mode (TEM) and the electron temperature gradient (ETG) mode. They differ in particular by their typical scale (e.g. their correlation length or equivalently the inverse of their wavenumber $1/k_{\perp}$).

Magnetohydrodynamic activity is also important for ITER. Tearing modes could trigger a loss of internal transport barriers. Moreover, the fast alpha particles could destabilized various forms of Alfvén eigenmodes that eject the fast alpha particles before thermalisation.

Experimental progress on all these issues needs diagnostics with high resolution in space, in time and able to probe different spatial scale. Derived from radar principle, reflectometry is a versatile density diagnostic using microwave [4, 5]. Reflectometry is now a routine density profile diagnostic.

This non-perturbative technique is able also to provide qualitative and quantitative measurements on density fluctuations over whole plasma. This paper presents some of the recent results obtained with reflectometry on particle transport, turbulence and MHD.

The article is organised as follows. Reflectometry principles are summarized in the second section. Particle transport is then addresses. The fourth section deals with turbulence observations, it covers the scaling of density fluctuations with β, the detection of zonal flows and the measurements at small scales. The next paragraph presents results on MHD. The article ends with a conclusion.

2. PRINCIPLE OF REFLECTOMETRY MEASUREMENTS

2.1 REFLECTOMETRY CUTOFF

Reflectometry measures the amplitude and the phase variation of a microwave reflected from a cut-off layer at a position that depends on the wave frequency, the polarisation and local parameter like the density. In the Ordinary polarization (O-mode) with E//B (where E is the wave electric field and B the plasma magnetic field) the cut-off corresponds to the plasma frequency $fp = \frac{1}{2\pi}\left(\frac{n_e e2}{\varepsilon_0 m_e}\right)^{0.5}$ and thus depends only on the electron density n_e.

The cut-off frequency for the extraordinary polarization (X-mode) for $E_{\perp}B$ waves, depends also on the magnetic field. There are two cut-off frequencies named upper f_R and lower f_L cut-off, $f_{R/L} = \frac{1}{2}\left(\sqrt{f_{ce}^{\,2} + 4f_p^{\,2}} \pm f_{ce}\right)$, where $f_{ce} = \frac{1}{2\pi}\frac{eB}{m_e}$ is the electron cyclotron frequency. The upper cut-off presents the advantages that the edge density can be probed since the cut-off frequency is finite $(f_R=f_{ce})$ at $n_e=0$. Owing to the magnetic field dependence, in tokamak, the center and the high field side can be also reached even with a flat density profile. However, strong absorption at the 2nd harmonic of electron cyclotron frequency limits core access at low magnetic field or in very high temperature plasmas.

2.2 PRINCIPLE OF MEASUREMENT

Phase and amplitude variations due to round trip into the plasma are monitored by comparison with a reference signal. The phase is the main quantity of interest while the amplitude shows the reflectivity variation due to geometrical effects. Using the WKB approximation [5], the main part of phase variation between antenna at $x=0$ and the reflecting layer at $x=r_{co}$ can be estimated:

$$\varnothing_p = \frac{4\pi}{c} \cdot f \cdot \int_{x=0}^{r_{co}} N(r, f, t)\, dr - \frac{\pi}{2} \qquad (1)$$

where $N(r,t)$ is the index of refraction and $-\pi/2$ is a correction due to the nature of the reflection.

A variation of the phase ϕ_p can result from a variation of the probing frequency or the optical path length between the antenna and the cut-off layer along the line of sight. Temporal changes of the phase can thus be written as:

$$\frac{\partial \Phi_p}{2} = \frac{4\pi}{c} \cdot \left(\frac{\partial f}{\partial t} \right) \cdot \int_{x=0}^{r_{co}} N(r, f, t)\, dr + \frac{4\pi}{c} \cdot f \cdot \frac{\partial}{\partial t} \left(\int_{x=0}^{r_{co}} N(r, f, \right. \quad (2)$$

The first term gives the optical path length, i.e. the position of the reflecting layer r_{co}, when the frequency f is swept, the second term turning negligible at current high sweeping rate (0.1 to 1GHz/s). The density profile is recovered using an inversion method.

The second term in equation (2) describes phase changes introduced by fluctuations of the optical path length arising from temporal and spatial fluctuations of the electron density. First, the beam is scattered all along its path by small scale fluctuations. The back scattering satisfies the Bragg rule $k_f = 2k(x)$ where k_f is the density fluctuation wave number and $k(x)$ the local wave number of the probing wave. The latter decreases from vacuum wave number at the edge to small value near the cut-off. However, in usual condition, large scale fluctuations (radial wave number $k_r < 3\ cm^{-1}$) at the vicinity of the cut-off layer masked the back scattering phase variation [6, 7]. Fixed-frequency reflectometer can then be seen as a monitor of the cut-off motion, which displays the time density perturbations in the plasma.

2.3 DOPPLER REFLECTOMETRY

Doppler reflectometry relies on the backscattering process. It was tested at the end of the 1990s [8] and it is now used on different magnetic fusion experiments [9, 10]. In Doppler reflectometry, the field backscattered along the beam path is separated from the field reflected at the cutoff layer (standard reflectometry) by launching the probing beam in oblique incidence with respect to the cutoff layer. The localized swelling of the incident field at the cutoff amplifies the scattering process and ensures some localization of the scattering process near the cutoff layer. The selected wavenumber and the localisation can be modified by varying the frequency or the incidence angle. Doppler reflectometry measures also the turbulence rotation velocity v_f though the frequency spectrum Doppler shift $\Delta\omega = k_f \bullet {}^r v_f$.

3 RESULTS ON PARTICLE TRANSPORT OBTAINED WITH REFLECTOMETRY

Particle transport analysis needs density profiles with good spatial and temporal resolution since the time evolution of the profile is needed to evaluate the diffusion coefficient D and the pinch velocity V, the particle flux being written $\Gamma_r = -D\nabla n_e + V n_e$ in the absence of particle source. Reflectometry able to measure with good spatial and temporal resolution the density profile is a key diagnostic for transport studies, like in the pedestal [11].

3.1 OBSERVATION OF A "MEXICAN HAT" LIKE STRUCTURE ON DENSITY PROFILE

On Tore-Supra, three X-mode reflectometers covering the band 50-155GHz measure the density profile from the edge to the high field Side (HFS) [12]. The core reflectometer can also operate at fixed frequency providing density profiles and density fluctuations in the same shot [13].

In the center, a local peaking, a feature that looks like a “Mexican hat”, is observed in ohmic shots, Figure 1(a). Using repetitive measurements -the dwell time between two profiles was reduced to 5μs- we were able to follow the time evolution, see [14] for more details. Starting from a flat density profile after a sawtooth crash, the density increases linearly on the magnetic axis during the recovery phase, while it remains flat around the q=1 surface. This peaking can represent up to 10% of the density on q=1, its width is typically 15cm, while the flat region extend beyond the q=1 surface. This structure is not seen on the temperature profile from ECE diagnostic.

3.2 TRANSPORT ANALYSIS OF THE MEXICAIN HAT

The inward pinch deduced from the density time evolution is around 0.1m/s, of the order of the neoclassical Ware pinch [15] (Fig.2). Observation of a lower peaking when decreasing the loop voltage with lower hybrid current drive confirms the role of the electric field and thus of the Ware pinch near the magnetic axis. This result is to be contrasted with the plasma behavior in the gradient zone, where the particle pinch has been shown to be turbulent [16].

The Ware pinch is sufficient to produce such a dense core because the diffusion coefficient is low, around 0.05 to 0.1 m2/s. This result is consistent with the very low level of density fluctuations that is measured inside the q=1 surface, as shown Fig.3. Vanishing of the peaked density with high ICRH power, density fluctuations are then much higher, shows that both the Ware pinch and a reduced particle diffusion are necessary to built this dense core.

3.3 RECENT TECHNICAL PROGRESS ENABLING THESE MEASUREMENTS

First broadband profile reflectometers were built with high voltage, high frequency sources that were very noisy. The sweeping time of the order of a millisecond was much larger than turbulence characteristic time. Reflectometers are now based on frequency multipliers and low frequency sources [17, 18]. The performances of these solid state components have increased tremendously driven by telecom industry. Solid state source can be swept in few microseconds. Decreasing the sweeping time to tens of microsecond range ‘‘freezes’’ the turbulence and substantially improves the profile reconstruction [19]. Broadband multiplier and amplifiers delivering above 10mW up to 110GHz are now commercialised. Up to 160GHz, the output power can reach few milliwatts. This frequency range approaches the highest frequency requires for ITER reflectometers. Solid state components help to improve performance and reliability of reflectometers.

4 TURBULENCE STUDIES

4.1 DENSITY FLUCTUATIONS DEPENDENCE WITH B

The ITER scaling law for the H-mode predict a strong degradation of the confinement time τE with the dimensionless parameter β. Dedicated experiments have shown contradicted results: on JET [20] and DIII-D [ ] a very weak dependence was found while JT-60U [22] shows a degradation in agreement with the ITER scaling. This contradiction is still unresolved, in particular the role of

ELM that are driven by MHD and thus β dependent remains unclear.

To avoid the pedestal contribution, a β-scaling experiment in L-mode was recently achieved on Tore-Supra [23]. The β profile was increased by a factor of 2 while keeping other dimensionless parameters. In addition to confinement time analysis, density fluctuations were also performed. The reflectometry accessibility allows an overlap of fluctuation profiles in the area $-0.5<r/a<0.5$. Figure 4 shows that outside the q=1 surface, the fluctuation level does not change with β, in agreement with the confinement time that shows a very weak degradation $\tau_E \mu \beta^{-0.3\pm0.1}$.

4.2 OBSERVATION OF ZONAL FLOWS AND GEOACOUSTIC MODES

Zonal flows are turbulence-generated time-varying rigid poloidal plasma flows. Experimental evidence of zonal flows and geodesic acoustic modes, the ZF high frequency class, has just emerged (see the special issue on experimental evidence of zonal flows [24]). ZF generate oscillations in the plasma radial electric field Er and thus in the local E × B velocity. On Asdex–Upgrade, these velocity oscillations were detected by Doppler reflectometry [25]. The Doppler velocity frequency spectrum exhibits a peak in the 20-50kHz range. Such a peak is only observed near the plasma edge. The frequency of this peak does not change with the density or the magnetic field, while a clear relation with the local temperature is observed, in agreement with GAM properties.

On T-10 tokamak, Melnikov et al, have measured GAM characteristic using correlation reflectometry [ ]. The observed mode has a m=0 poloidal number and its radial correlation length of a few centimetres. Correlation reflectometry was also able to detect GAM in the plasma core, and their position may be connected with low order rational surfaces *q = 1, 1.5, 2, 3, 4*.

4.3 FLUCTUATION MEASUREMENT AT SMALL SCALES

4.3.1 Poloidal k spectrum

The large scale (ITG, TEM) modes are believed to be responsible for the major part of the transport. In internal transport barrier regime, a reduction of the largest scale turbulence is observed while the electron transport channel remains at high level. This transport could be due to ETG [ ], showing the benefit to measure fluctuations from large to small scale.

Doppler reflectometry has such capability. On Tore-Supra, the Doppler reflectometer can perform a double scan for tilt angle and frequency to measure the $k_\perp$-spectrum at various positions [28]. In Ohmic regime, the level of fluctuations is found to be much lower than expected on the basis a Kraichnan law k_θ^{-3}, which characterizes the spectrum at low wave numbers. This measurement is in fair agreement with previous observations done with the laser coherent diffusion diagnostic ALTAIR [ ]. It turns out that the whole spectrum (low and high wave numbers) is well described by an exponential decay $S(k_\theta) \propto (\exp -4k_\theta \varrho_i)$, where ϱ_i is the ion Larmor radius, see Fig.5. This observation suggests a minor role of Electron Temperature Gradient driven modes in these plasmas.

4.3.2 Density fluctuations properties from fast swept reflectometers

While Doppler reflectometry measures mainly the perpendicular spectrum, the radial wavenumber kr-spectrum could be measured from fast swept reflectometry [30]. Using repetitive sweeps, the average phase variation due to the equilibrium profile can be eliminated. The remaining phase fluctuations comes from back-scattering along the beam path at $k_r=2k(x)$ (Bragg rule). With a Fourier transform of the phase fluctuations, we can access the radial wavenumber kr-spectrum of density fluctuations. Using a sliding radial windows, we can determine the local radial wavenumber kr spectrum and the profile of density fluctuations by integrating the kr-spectrum. This method was assessed with full-wave simulations [31].

However, high level fluctuations at the edge generate non-linear effects that distort the spectrum. The energy is conserved, meaning that the fluctuation level measurements are not affected numerical simulations or comparison with fixed frequency measurement show [32]. From numerical simulations it could be possible to establish a method to correct the nonlinear effects.

5 RESULTS ON MHD

5.1 OBSERVATION OF TEARING MODES

On tokamaks, tearing-like Magneto Hydrodynamic Modes (MHD) modes can developed on low rational surfaces. Such modes flatten locally the density profile and can thus be detected with reflectometry [33]. On Tore-Supra, Vermare et al were able to localise the mode and follow its time evolution using repetitive fast sweep [34].

5.2 OBSERVATION OF ALVÈN MODES

High frequency MHD modes like the Alfvén modes can also be detected though the density perturbations they induced. Various classes of Alfvén eigen modes can be destabilized by energetic ions, see for Fig.6. Alfvén cascades (AC) are observed in reversed sheare plasmas. The AC frequency traces the evolution of the minimal q value. On JET, using O-mode reflectometer in the interferometry regime, it was possible to monitor the evolution of the safety factor and density of rational magnetic surfaces in the region of maximum plasma current, a method called MHD spectroscopy [35]. Although the interfometry regime does not give any localisation, numerical reconstruction of the phase evolution agrees with an AC localisation on the high field side [36].

On Tore-Supra, in combined ICRH and LH heated discharges, two classes of coherent modes have been observed with fixed frequency reflectometry. The high frequency branch, in the range 100-150kHz, was identified as a toroidal Alfven eigen Mode (TAEs) [37]. A lower branch in the range 20-80kHz can also be detected. These modes are detected over a large fraction of the plasma, but the radial variation of the density fluctuations shows that both modes are localised at the same position on the high field side, see Fig.7. Such anti-balloning structure was also observed in TFTR for TAEs [38]. Although the low frequency range lies within range of acoustic frequencies, these observations exclude the GAM. Owing to the similary with the TAE, these modes are likely Beta Alfvén Eigenmodes (BAEs) that follows same dispersion relation as the GAM, but their spatial

structure is different [39].

CONCLUSION

New reflectometry method and the technical progress have made reflectometry a reliable and very powerful diagnostic technique. The different reflectometry methods offer a multi-tools to analyze particle transport, turbulence and MHD. Profile reflectometry can measure the density profile and tearing modes. Fixed frequency measurements is adapted to large scale perturbations. Doppler reflectometry can probe the small scale, and though the Doppler effect can also detect the ZF. Lastly, correlation reflectometry investigates the spatial structure of the perturbations.

Combining the reflectometry methods should ensure further progress. Profile and fluctuation measurement was essential to explain the origin of the "Mexican hat". Determining the underlying instabilities requires to look from large to small scale instabilities.

REFERENCES

[1]. Horton W 1999, Rev. Mod. Phys. **71** 735

[2]. Garbet X 2004 Plasma Phys. Control Fusion **46** B557

[3]. P H Diamond, S-I Itoh, K Itoh and T S Hahm, Plasma Phys. Control. Fusion **47**, R35 (2005).

[4]. E. Mazzucato, Rev. Sci. Instrum. **69**, 2201 (1998).

[5]. H. J. Hartfuss, T. Geist and M. Hirsh, Plasma Phys. Control. Fusion **39**, 1693 (1997).

[6]. Bretz N 1992 Phys. Fluids B **4** 2414

[7]. C Fanack et al., Plasma Phys. Control. Fusion **38**, 1915 (1996).

[8]. M. Hirsch et al., Rev. Sci. Instrum. 72, 324 (2001).

[9]. Conway G D, Schirmer J, Klenge S, Suttrop W, Holzhauer E and ASDEX Upgrade Team 2004 Plasma Phys. Control. Fusion **46** 951

[10]. P. Hennequin et al., Rev. Sci. Instrum., **75**, 3881 (2004)

[11]. Zeng L. et al 2003 Plasma Phys. Control. Fusion **46** A121

[12]. R. Sabot et al., Int. J. Infrared Millim. Waves 25, 229 (2004).

[13]. R. Sabot, A. Sirinelli, J.-M. Chareau, and J.-C. Giacalone, submitted to Nuclear Fusion.

[14]. Sirinelli A., Sabot R, Garbet X, Bourdelle C, Giacalone J C, Hoang G T, Ségui J L and Hennequin P to be submitted to Phys. Rev. Lett.

[15]. Ware A A 1970 Physical Review Letters **25**, 15

[16]. G. T. Hoang et al., Phys. Rev. Lett. **90**, 155002 (2003)

[17]. A. Silva et al. Rev. Sci. Instrum. **70**, 1072 (1999)

[18]. F. Clairet, at al., Rev. Sci. Instrum., 74, 1481, (2003).

[19]. Moreau Ph, Clairet F, Chareau J-M, Paume M and Laviron C 200 Rev. Sci. Instrum. **71** 74

[20]. McDonald D C et al 2004 Plasma Phys. Control. Fusion **48**,A215

[21]. Pety C C et al, 2004 Phys.Plasma **11**,5

[22]. Urano et al, to be published in Nuclear Fusion
[23]. Sirinelli A et al. in 33rd EPS Conference on Controlled Fusion and Plasma Physics, Roma, 2006.
[24]. Plasma Phys. Control. Fusion 2006, **48**, S1-S212, edited by S-I Itoh
[25]. Conway G D, Scott B, Schirmer J, Reich M, Kendl A and ASDEX Upgrade Team 2005 Plasma Phys. Control. Fusion **47** 1165
[26]. Melnikov A V et al 2006 Plasma Phys. Control. Fusion **48** S87–S110
[27]. Stallard B W et al 1999 Phys. Plasmas **6** 1978
[28]. P. Hennequin et al., Rev. Sci. Instrum., **75**, 3881 (2004)
[29]. P. Hennequin at al **46**, B121–B133 (2004)
[30]. Heuraux S, Hacquin S, da Silva F, Clairet F, Sabot R and Leclert G 2003 Rev. Sci. Instrum. **74** 1501
[31]. Vermare L, Heuraux S, Clairet F, Leclert G and da Silva P submitted to Nuclear Fusion.
[32]. Gerbaud T, Clairet F, Heuraux S, Sirinelli A, Vermare L, Sabot R, submitted to Rev. Sci. Instrum.
[33]. Conway G D et al 2002 28th EPS Conf. on Controlled Fusion and Plasma Physics (Montreux) vol 26B (ECA)
[34]. L. Vermare et al., accepted for publication in Plasma Phys. Control. Fusion **47** (2005).
[35]. Sharapov S E et al 2005 Phys. Rev. Lett. **93**, 165001
[36]. Hacquin S et al in 33rd EPS Conference on Controlled Fusion and Plasma Physics, Roma, 2006.

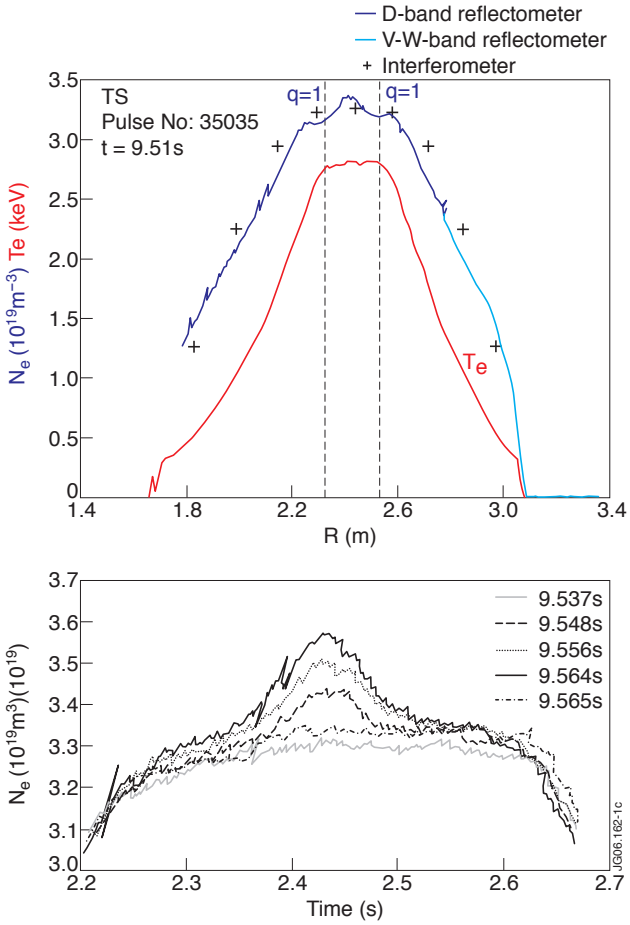

Figure 1: a) Density profile from reflectometry (50-110 GHz thin, 105-155GHz thick) and interferometry (crosses) for an ohmic shot. The temperature profile is shown and the dot lines show the position of q=1 surface.
b) Time evolution of the central peaking (same shot as 4a). The central profile is flat after the sawtooth crash (t=9.537), the local peaking grows during the sawtooth period, before vanishing after the crash (t=9.565).

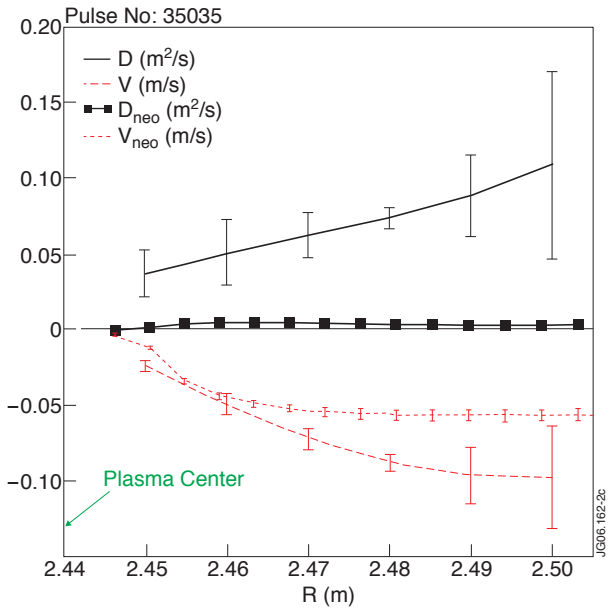

Figure 2: Pinch velocity V and particle transport coefficient D measured from experimental density profiles and neoclassical values from NCLASS transport code.

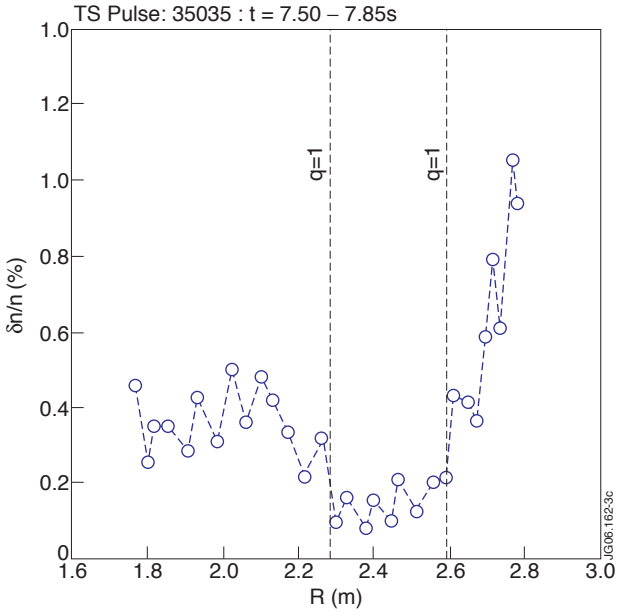

Figure 3: Density fluctuation profile showing a drop of fluctuation inside the q=1 surface.

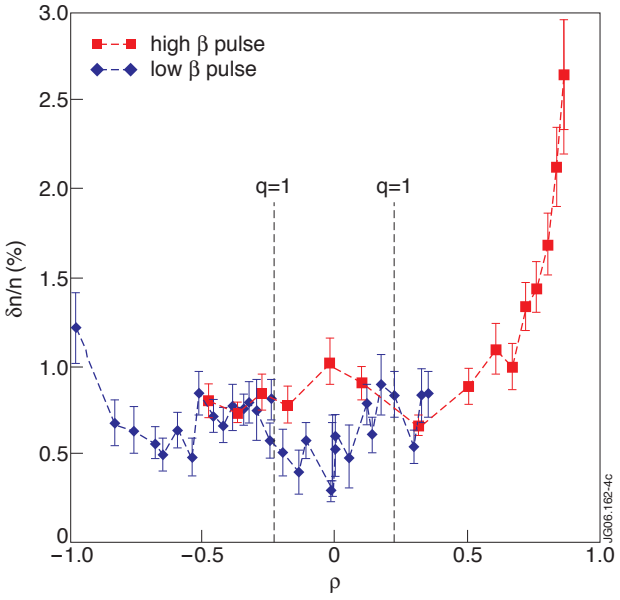

Figure 4: Fluctuation profile in the high and low β pulses.

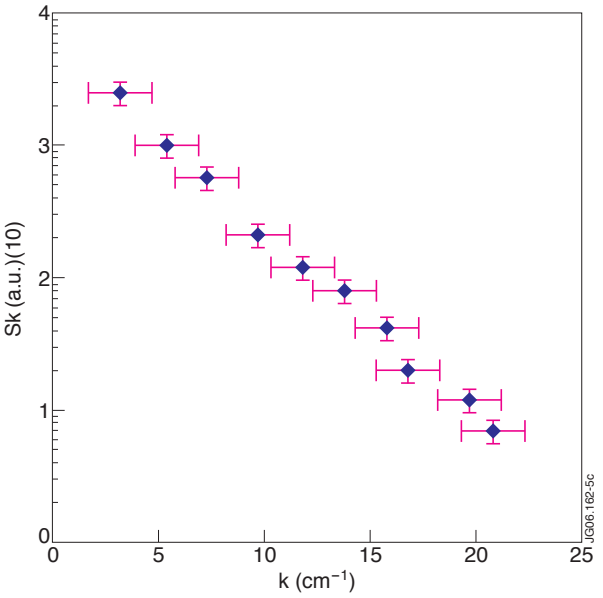

Figure 5: k spectrum of density fluctuations in ohmic regime, at mid-radius.

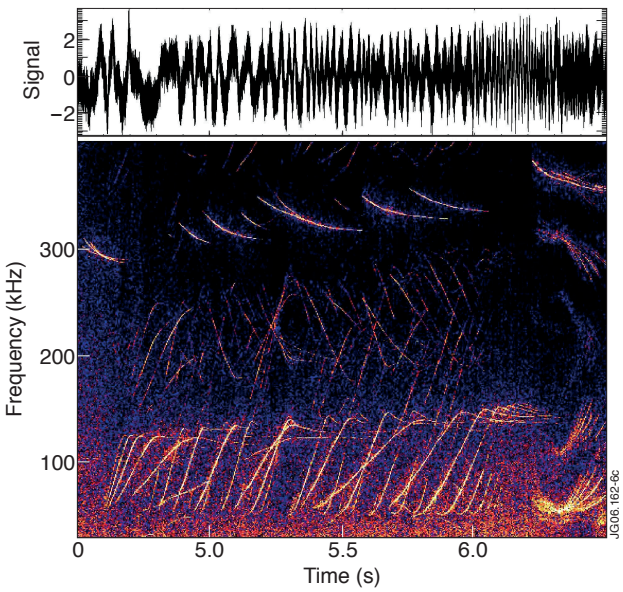

Figure 6: Exemple of various forms of Alven modes in JET, 40-150kHz: TAE and AC, 300-400kHz Elliptical Alfvén eigen modes.

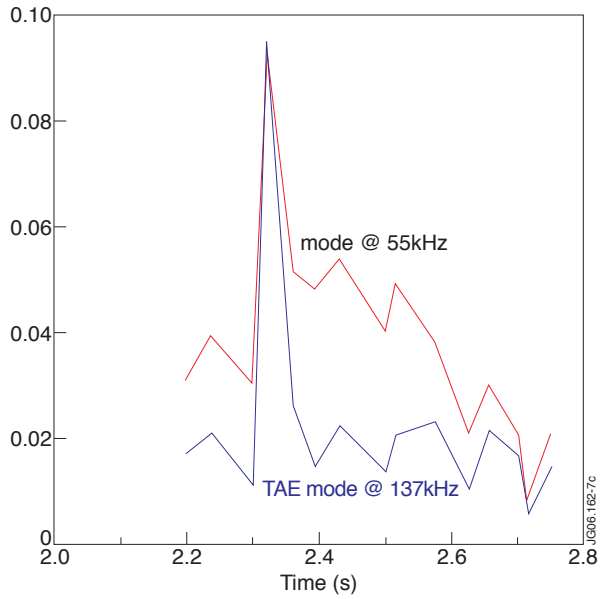

Figure 7: Radiale profile of the density fluctuations amplitude induced by the low frequency modes (red) and the TAE mode (the frequency spectrum is inserted).